Electronic Supplementary Material

Construction of single atom copper loaded iron-based MOF/carbon nitride nanosheet heterojunction for enhanced N_2 photofixation under visible light

Xinshan Rong (✉), Yuqing He, Ping Gao, Ting Sun, Xiangtong Zhou, and Zhiren Wu (✉)

School of Environment and Safety Engineering, Jiangsu University, Zhenjiang 212013, China

E-mails: rxsmile@ujs.edu.cn (X.R.), zhirenwu@126.com (Z.W.)

Characterization

Morphologies of all photocatalyst samples were observed using a scanning electron microscope (SEM; JSM-7800F, JEOL). Microstructures of materials were characterized by a transmission electron microscope (TEM; JEM-2100). High-angle annular dark-field scanning transmission electron microscopy (HAADF-STEM) was carried out using a high-resolution transmission electron microscope (HRTEM; FEI Titan G2 60–300). Element analyses of samples were conducted on the FEI Tecnai G2 S-Tw instrument equipped with an energy dispersive X-ray spectrometer (EDX). The content of Cu was quantified by an Optima 7300 DV inductively coupled plasma atomic emission spectrometer (ICP-AES). X-ray diffraction (XRD) patterns were measured using a D/MAX-2500 diffractometer taking Cu Kα as a radiation source (λ = 0.15418 nm). The scanning range was 5°–80° at 40 kV and 40 mA, with the scanning rate of 6(°)/min. An ESCALAB 250Xi instrument was used to carry out X-ray photoelectron spectroscopy (XPS), measuring analytical compositions and surface properties. Photogenerated electron–hole pair recombination rates of prepared catalysts were measured through photoluminescence (PL) spectroscopy using a fluorescence spectrophotometer (F-4600, Hitachi, Japan). Brunauer–Emmett–Teller (BET) specific surface area (SSA) values were determined using a ASAP 2020 M micromeritics system. Diffuse reflectance spectroscopy (DRS) was performed on a TU-1901 ultraviolet–visible (UV–Vis) spectrophotometer using $BaSO_4$ as the reflectance standard. Photoelectrochemical (PEC) measurements were conducted on a CHI660 electrolysis workstation using 0.1 mol·L^{-1} sodium sulfate as the electrolyte.

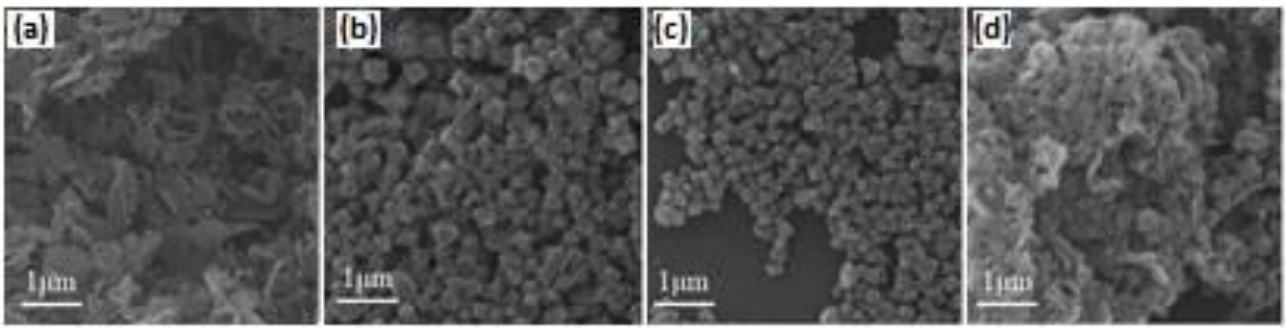

Fig. S1 SEM images of **(a)** NCN, **(b)** Fe-MOF, **(c)** Cu@MIL, and **(d)** Cu@MIL-NCN-3.

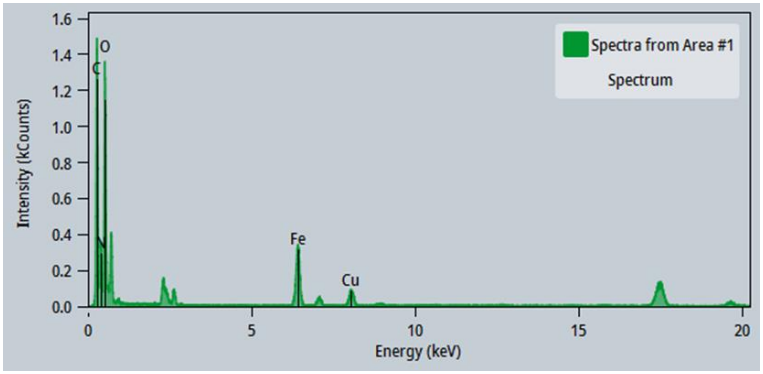

Fig. S2 Total spectrum of EDX surface of Cu@MIL-NCN-3.

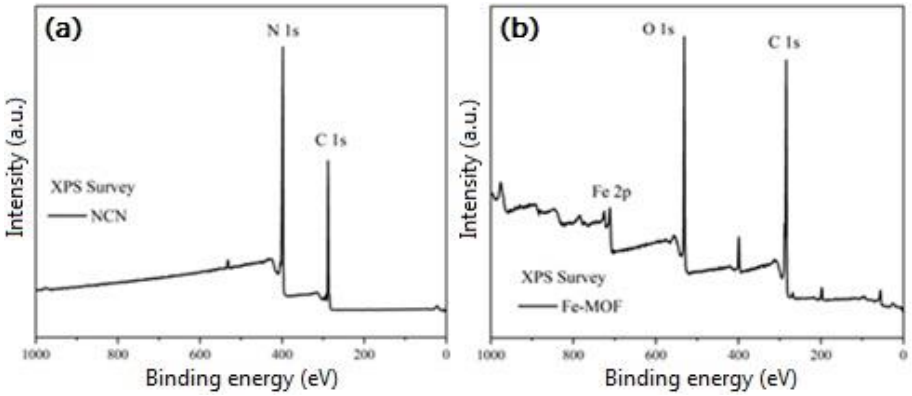

Fig. S3 XPS survey spectra of **(a)** NCN and **(b)** Fe-MOF.

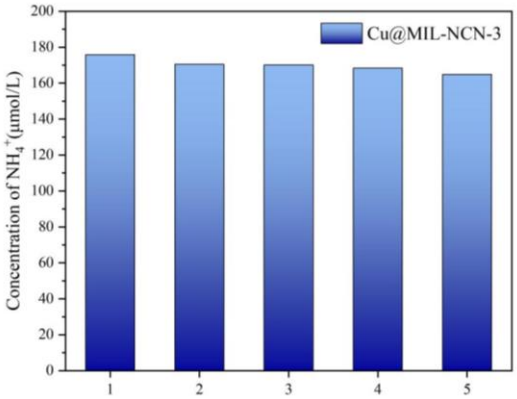

Fig. S4 Production of NH_3 on Cu@MIL-NCN-3 corresponding to the recycling run.

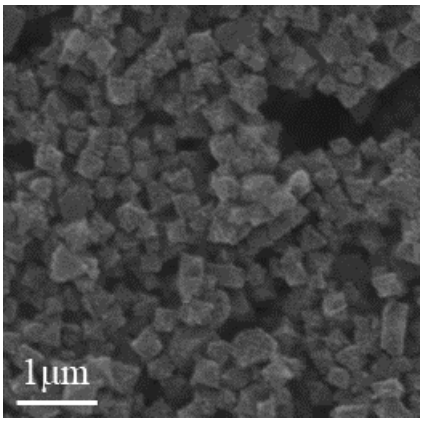

Fig. S5 SEM image of Cu@MIL-NCN-3 after nitrogen fixation reaction.

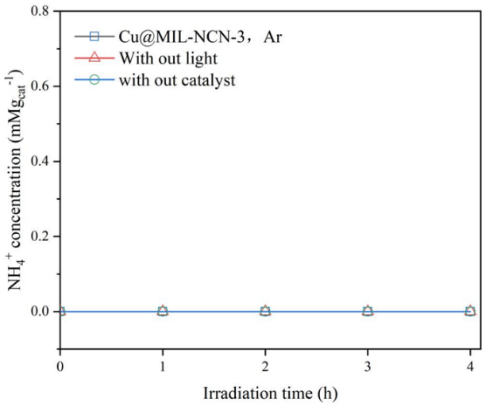

Fig. S6 Control experiment results for photocatalytic N_2 fixation reactions.

Table S1 Comparison of N_2 photofixation rates with various photocatalysts

Photocatalyst	Scavenger	N_2 photofixation rate/($\mu mol \cdot g^{-1} \cdot h^{-1}$)	Ref.
Cu@MIL-NCN-3	None	175.83	This study
MIL-125@TiO_2	None	102.70	[1]
Au@UiO-66	None	18.90	[2]
Ti_3C_2-QD/Ni-MOF	Na_2SO_3	88.79	[3]
ZIF-67@PMo_4V_8	None	149.0	[4]

References

[1] Wang L, Wang S, Li M, et al. Constructing oxygen vacancies and linker defects in MIL-125@TiO_2 for efficient photocatalytic nitrogen fixation. Journal of Alloys and Compounds, 2022, 909: 164751

[2] Chen L-W, Hao Y-C, Guo Y, et al. Metal–organic framework membranes encapsulating gold nanoparticles for direct plasmonic photocatalytic nitrogen fixation. Journal of the American Chemical Society, 2021, 143(15): 5727–5736

[3] Qin J, Liu B, Lam K-H, et al. 0D/2D MXene quantum dot/Ni-MOF ultrathin nanosheets for enhanced N_2 photoreduction. ACS Sustainable Chemistry & Engineering, 2020, 8(48): 17791–17799

[4] Li X H, He P, Wang T, et al. Keggin-type polyoxometalate-based ZIF-67 for enhanced photocatalytic nitrogen fixation. ChemSusChem, 2020, 13(10): 2769–2778